Phys. Lett. B 854 (2024) 138715

Contents lists available at ScienceDirect

Physics Letters B

journal homepage: www.elsevier.com/locate/physletb

Letter

Measurements of the Z^0/γ^* cross section and transverse single spin asymmetry in 510 GeV p+p collisions

The STAR Collaboration

M.I. Abdulhamid [d], B.E. Aboona [bd], J. Adam [p], L. Adamczyk [b], J.R. Adams [ao], I. Aggarwal [aq], M.M. Aggarwal [aq], Z. Ahammed [bk], E.C. Aschenauer [f], S. Aslam [ab], J. Atchison [a], V. Bairathi [bb], J.G. Ball Cap [x], K. Barish [k], R. Bellwied [x], P. Bhagat [ae], A. Bhasin [ae], S. Bhatta [ba], S.R. Bhosale [s], J. Bielcik [p], J. Bielcikova [an], J.D. Brandenburg [ao], C. Broodo [x], X.Z. Cai [ay], H. Caines [bo], M. Calderón de la Barca Sánchez [i], D. Cebra [i], J. Ceska [p], I. Chakaberia [ah], P. Chaloupka [p], B.K. Chan [j], Z. Chang [ac], A. Chatterjee [r], D. Chen [k], J. Chen [ax], J.H. Chen [u], Z. Chen [ax], J. Cheng [bf], Y. Cheng [j], S. Choudhury [u], W. Christie [f], X. Chu [f,*], H.J. Crawford [h], M. Csanád [s], G. Dale-Gau [m], A. Das [p], I.M. Deppner [w], A. Dhamija [aq], P. Dixit [z], X. Dong [ah], J.L. Drachenberg [a], E. Duckworth [af], J.C. Dunlop [f], J. Engelage [h], G. Eppley [as], S. Esumi [bg], O. Evdokimov [m], O. Eyser [f], R. Fatemi [ag], S. Fazio [g], C.J. Feng [am], Y. Feng [ar], E. Finch [az], Y. Fisyak [f], F.A. Flor [bo], C. Fu [ad], C.A. Gagliardi [bd], T. Galatyuk [q], T. Gao [ax], F. Geurts [as], N. Ghimire [bc], A. Gibson [bj], K. Gopal [aa], X. Gou [ax], D. Grosnick [bj], A. Gupta [ae], W. Guryn [f], A. Hamed [d], Y. Han [as], S. Harabasz [q], M.D. Harasty [i], J.W. Harris [bo], H. Harrison-Smith [ag], W. He [u], X.H. He [ad], Y. He [ax], N. Herrmann [w], L. Holub [p], C. Hu [bh], Q. Hu [ad], Y. Hu [ah], H. Huang [am], H.Z. Huang [j], S.L. Huang [ba], T. Huang [m], X. Huang [bf], Y. Huang [bf], Y. Huang [l], T.J. Humanic [ao], M. Isshiki [bg], W.W. Jacobs [ac], A. Jalotra [ae], C. Jena [aa], A. Jentsch [f], Y. Ji [ah], J. Jia [f,ba], C. Jin [as], X. Ju [au], E.G. Judd [h], S. Kabana [bb], D. Kalinkin [ag], K. Kang [bf], D. Kapukchyan [k], K. Kauder [f], D. Keane [af], A. Khanal [bm], Y.V. Khyzhniak [ao], D.P. Kikoła [bl], D. Kincses [s], I. Kisel [t], A. Kiselev [f], A.G. Knospe [ai], H.S. Ko [ah], L.K. Kosarzewski [ao], L. Kumar [aq], M.C. Labonte [i], R. Lacey [ba], J.M. Landgraf [f], J. Lauret [f], A. Lebedev [f], J.H. Lee [f], Y.H. Leung [w], N. Lewis [f], C. Li [ax], D. Li [au], H.-S. Li [ar], H. Li [bn], W. Li [as], X. Li [au], Y. Li [au], Y. Li [bf], Z. Li [au], X. Liang [k], Y. Liang [af], R. Licenik [an,p], T. Lin [ax], Y. Lin [v], M.A. Lisa [ao], C. Liu [ad], G. Liu [av], H. Liu [l], L. Liu [l], T. Liu [bo], X. Liu [ao], Y. Liu [bd], Z. Liu [l], T. Ljubicic [as], O. Lomicky [p], R.S. Longacre [f], E.M. Loyd [k], T. Lu [ad], J. Luo [au], X.F. Luo [l], L. Ma [u], R. Ma [f], Y.G. Ma [u], N. Magdy [ba], D. Mallick [bl], R. Manikandhan [x], S. Margetis [af], C. Markert [be], G. McNamara [bm], O. Mezhanska [p], K. Mi [l], S. Mioduszewski [bd], B. Mohanty [al], M.M. Mondal [al], I. Mooney [bo], J. Mrazkova [an,p], M.I. Nagy [s], A.S. Nain [aq], J.D. Nam [bc], M. Nasim [z], D. Neff [j], J.M. Nelson [h], D.B. Nemes [bo], M. Nie [ax], G. Nigmatkulov [m], T. Niida [bg], T. Nonaka [bg], G. Odyniec [ah], A. Ogawa [f], S. Oh [aw], K. Okubo [bg], B.S. Page [f], R. Pak [f], S. Pal [p], A. Pandav [ah], A.K. Pandey [ad], T. Pani [at], A. Paul [k], B. Pawlik [ap], D. Pawlowska [bl], C. Perkins [h], J. Pluta [bl], B.R. Pokhrel [bc], M. Posik [bc], T. Protzman [ai], V. Prozorova [p], N.K. Pruthi [aq], M. Przybycien [b], J. Putschke [bm], Z. Qin [bf], H. Qiu [ad], C. Racz [k], S.K. Radhakrishnan [af], A. Rana [aq], R.L. Ray [be],

* Corresponding author.
E-mail address: xchu@bnl.gov (X. Chu).
* Deceased.

https://doi.org/10.1016/j.physletb.2024.138715
Received 28 August 2023; Received in revised form 8 May 2024; Accepted 9 May 2024
Available online 21 May 2024

R. Reed [ai], C.W. Robertson [ar], M. Robotkova [an,p], M.A. Rosales Aguilar [ag], D. Roy [at], P. Roy Chowdhury [bl], L. Ruan [f], A.K. Sahoo [z], N.R. Sahoo [aa], H. Sako [bg], S. Salur [at], S. Sato [bg], B.C. Schaefer [ai], W.B. Schmidke [f,*], N. Schmitz [aj], F.-J. Seck [q], J. Seger [o], R. Seto [k], P. Seyboth [aj], N. Shah [ab], P.V. Shanmuganathan [f], T. Shao [u], M. Sharma [ae], N. Sharma [z], R. Sharma [aa], S.R. Sharma [aa], A.I. Sheikh [af], D. Shen [ax], D.Y. Shen [u], K. Shen [au], S.S. Shi [l], Y. Shi [ax], Q.Y. Shou [u], F. Si [au], J. Singh [aq], S. Singha [ad], P. Sinha [aa], M.J. Skoby [e,ar], N. Smirnov [bo], Y. Söhngen [w], Y. Song [bo], B. Srivastava [ar], T.D.S. Stanislaus [bj], M. Stefaniak [ao], D.J. Stewart [bm], Y. Su [au], M. Sumbera [an], C. Sun [ba], X. Sun [ad], Y. Sun [au], Y. Sun [y], B. Surrow [bc], M. Svoboda [an,p], Z.W. Sweger [i], A.C. Tamis [bo], A.H. Tang [f], Z. Tang [au], T. Tarnowsky [ak], J.H. Thomas [ah], A.R. Timmins [x], D. Tlusty [o], T. Todoroki [bg], S. Trentalange [j], P. Tribedy [f], S.K. Tripathy [bl], T. Truhlar [p], B.A. Trzeciak [p], O.D. Tsai [j,f], C.Y. Tsang [af,f], Z. Tu [f], J. Tyler [bd], T. Ullrich [f], D.G. Underwood [c,bj], I. Upsal [au], G. Van Buren [f], J. Vanek [f], I. Vassiliev [t], V. Verkest [bm], F. Videbæk [f], S.A. Voloshin [bm], F. Wang [ar], G. Wang [j], J.S. Wang [y], J. Wang [ax], K. Wang [au], X. Wang [ax], Y. Wang [au], Y. Wang [l], Y. Wang [bf], Z. Wang [ax], J.C. Webb [f], P.C. Weidenkaff [w], G.D. Westfall [ak], D. Wielanek [bl], H. Wieman [ah], G. Wilks [m], S.W. Wissink [ac], R. Witt [bi], J. Wu [l], J. Wu [ad], X. Wu [j], X. Wu [au], B. Xi [u], Z.G. Xiao [bf], G. Xie [bh], W. Xie [ar], H. Xu [y], N. Xu [ah], Q.H. Xu [ax], Y. Xu [ax], Y. Xu [l], Z. Xu [af], Z. Xu [j], G. Yan [ax], Z. Yan [ba], C. Yang [ax], Q. Yang [ax], S. Yang [av], Y. Yang [am], Z. Ye [as], Z. Ye [ah], L. Yi [ax], K. Yip [f], Y. Yu [ax], H. Zbroszczyk [bl], W. Zha [au], C. Zhang [u], D. Zhang [av], J. Zhang [ax], S. Zhang [n], W. Zhang [av], X. Zhang [ad], Y. Zhang [ad], Y. Zhang [au], Y. Zhang [ax], Y. Zhang [l], Z.J. Zhang [am], Z. Zhang [f], Z. Zhang [m], F. Zhao [ad], J. Zhao [u], M. Zhao [f], J. Zhou [au], S. Zhou [l], Y. Zhou [l], X. Zhu [bf], M. Zurek [c,f], M. Zyzak [t]

[a] *Abilene Christian University, Abilene, Texas 79699*
[b] *AGH University of Krakow, FPACS, Cracow 30-059, Poland*
[c] *Argonne National Laboratory, Argonne, Illinois 60439*
[d] *American University in Cairo, New Cairo 11835, Egypt*
[e] *Ball State University, Muncie, Indiana, 47306*
[f] *Brookhaven National Laboratory, Upton, New York 11973*
[g] *University of Calabria & INFN-Cosenza, Rende 87036, Italy*
[h] *University of California, Berkeley, California 94720*
[i] *University of California, Davis, California 95616*
[j] *University of California, Los Angeles, California 90095*
[k] *University of California, Riverside, California 92521*
[l] *Central China Normal University, Wuhan, Hubei 430079*
[m] *University of Illinois at Chicago, Chicago, Illinois 60607*
[n] *Chongqing University, Chongqing, 401331*
[o] *Creighton University, Omaha, NE 68178*
[p] *Czech Technical University in Prague, FNSPE, Prague 115 19, Czech Republic*
[q] *Technische Universität Darmstadt, Darmstadt 64289, Germany*
[r] *National Institute of Technology Durgapur, Durgapur - 713209, India*
[s] *ELTE Eötvös Loránd University, Budapest, H-1117, Hungary*
[t] *Frankfurt Institute for Advanced Studies FIAS, Frankfurt 60438, Germany*
[u] *Fudan University, Shanghai, 200433*
[v] *Guangxi Normal University, Guilin, 541004*
[w] *University of Heidelberg, Heidelberg 69120, Germany*
[x] *University of Houston, Houston, Texas 77204*
[y] *Huzhou University, Huzhou, Zhejiang 313000*
[z] *Indian Institute of Science Education and Research (IISER), Berhampur 760010, India*
[aa] *Indian Institute of Science Education and Research (IISER) Tirupati, Tirupati 517507, India*
[ab] *Indian Institute Technology, Patna, Bihar 801106, India*
[ac] *Indiana University, Bloomington, Indiana 47408*
[ad] *Institute of Modern Physics, Chinese Academy of Sciences, Lanzhou, Gansu 730000*
[ae] *University of Jammu, Jammu 180001, India*
[af] *Kent State University, Kent, Ohio 44242*
[ag] *University of Kentucky, Lexington, Kentucky 40506-0055*
[ah] *Lawrence Berkeley National Laboratory, Berkeley, California 94720*
[ai] *Lehigh University, Bethlehem, Pennsylvania 18015*
[aj] *Max-Planck-Institut für Physik, Munich 80805, Germany*
[ak] *Michigan State University, East Lansing, Michigan 48824*
[al] *National Institute of Science Education and Research, HBNI, Jatni 752050, India*
[am] *National Cheng Kung University, Tainan 70101*
[an] *Nuclear Physics Institute of the CAS, Rez 250 68, Czech Republic*
[ao] *The Ohio State University, Columbus, Ohio 43210*
[ap] *Institute of Nuclear Physics PAN, Cracow 31-342, Poland*
[aq] *Panjab University, Chandigarh 160014, India*
[ar] *Purdue University, West Lafayette, Indiana 47907*
[as] *Rice University, Houston, Texas 77251*
[at] *Rutgers University, Piscataway, New Jersey 08854*
[au] *University of Science and Technology of China, Hefei, Anhui 230026*
[av] *South China Normal University, Guangzhou, Guangdong 510631*

[aw] Sejong University, Seoul, 05006, South Korea
[ax] Shandong University, Qingdao, Shandong 266237
[ay] Shanghai Institute of Applied Physics, Chinese Academy of Sciences, Shanghai 201800
[az] Southern Connecticut State University, New Haven, Connecticut 06515
[ba] State University of New York, Stony Brook, New York 11794
[bb] Instituto de Alta Investigación, Universidad de Tarapacá, Arica 1000000, Chile
[bc] Temple University, Philadelphia, Pennsylvania 19122
[bd] Texas A&M University, College Station, Texas 77843
[be] University of Texas, Austin, Texas 78712
[bf] Tsinghua University, Beijing 100084
[bg] University of Tsukuba, Tsukuba, Ibaraki 305-8571, Japan
[bh] University of Chinese Academy of Sciences, Beijing, 101408
[bi] United States Naval Academy, Annapolis, Maryland 21402
[bj] Valparaiso University, Valparaiso, Indiana 46383
[bk] Variable Energy Cyclotron Centre, Kolkata 700064, India
[bl] Warsaw University of Technology, Warsaw 00-661, Poland
[bm] Wayne State University, Detroit, Michigan 48201
[bn] Wuhan University of Science and Technology, Wuhan, Hubei 430065
[bo] Yale University, New Haven, Connecticut 06520

ARTICLE INFO

Editor: H. Gao

Keywords:
Z^0
Cross section
Transverse momentum dependent parton distribution functions (TMDs)
Transverse single spin asymmetry (TSSA, A_N)
Sivers function

ABSTRACT

The differential cross section for Z^0 production, measured as a function of the boson's transverse momentum (p_T), provides important constraints on the evolution of the transverse momentum dependent parton distribution functions (TMDs). The transverse single spin asymmetry (TSSA) of the Z^0 is sensitive to one of the polarized TMDs, the Sivers function, which is predicted to have the opposite sign in $p + p \to W/Z + X$ from that which enters in semi-inclusive deep inelastic scattering. In this Letter, the STAR Collaboration reports the first measurement of the Z^0/γ^* differential cross section as a function of its p_T in p+p collisions at a center-of-mass energy of 510 GeV, together with the Z^0/γ^* total cross section. We also report the measurement of Z^0/γ^* TSSA in transversely polarized p+p collisions at 510 GeV.

1. Introduction

The internal structure of hadrons, described by their parton distribution functions (PDFs) [1], is an important topic in theoretical, phenomenological, and experimental studies in nuclear physics. During the past decades, numerous efforts have been made to understand transverse momentum dependent parton distribution functions (TMDs) [2] which encode both the parton's longitudinal momentum fraction (x) and its intrinsic transverse momentum (k_T). TMDs depict the density of partons in three dimensions [3,4], providing more detailed information on hadron structure than the one-dimensional collinear PDFs. There are eight leading-twist TMDs that are allowed by parity invariance [5] of Quantum Chromodynamics (QCD). Many observables in hard scattering experiments involving hadrons are related to TMDs. Utilizing factorization theorems, TMDs can be extracted through global fits of the cross section and other observables.

Observables related to TMDs require the measured transverse momentum component to be much smaller than the hard scale of the process. In semi-inclusive deep inelastic scattering (SIDIS), the hard scale is characterized by the square of the 4-momentum of the exchanged virtual photon ($Q^2 = -q^2$). If the measured transverse momentum of the outgoing hadron is small, $p_T^h \ll Q$, then TMD factorization can be applied. TMDs can also be extracted from di-lepton production in Drell-Yan (DY) events [6] if the transverse momentum of the lepton pair is sufficiently small, $q_T \ll Q$. In the Z^0 production events, Q^2 is the square of the Z^0 boson mass. On one hand, measuring the differential cross section as a function of transverse momentum for different processes tests the universality of TMDs and provides opportunities to study their Q^2 evolution. Measurements of $p+p \to Z^0/\gamma^*$ at STAR complement the results of SIDIS at the HERMES [7] and COMPASS [8,9] experiments and DY/Z^0 production at the E288 [10], E605 [11], E772 [12], CDF [13–16], D0 [17–19], ATLAS [20–22], CMS [23–25], LHCb [26–28], COMPASS [29], and PHENIX [30] experiments. On the other hand, studying the $p + p \to Z^0/\gamma^*$ process at the intermediate energies available at RHIC provides access to a high x region.

In addition to the unpolarized measurements, RHIC opens a window to explore the polarized TMDs through transversely polarized p+p collisions. Of particular interest is the Sivers function ($f_{1T}^{\perp}$) [31,32], which describes the unpolarized parton distribution inside a transversely polarized proton. High precision experimental data are needed to determine $f_{1T}^{\perp}$ as current results extracted by different groups still show fairly large uncertainties for $f_{1T}^{\perp}$ [33–35], especially in the relatively high x region ($x \geq 0.1$) probed by RHIC data. There are non-trivial predictions for the process dependence of the Sivers function stemming from gauge invariance. In SIDIS, the Sivers function is associated with a final-state effect through gluon exchange between the struck parton and the target nucleon remnants. In p+p collisions, however, the Sivers asymmetry originates from the initial state of the interaction for the DY process and $W^{\pm}/Z^0$ boson production. As a consequence, the gauge invariant definition of the Sivers function predicts the opposite sign for the Sivers function in SIDIS compared to processes with color charges in the initial state and a colorless final state, such as $p + p \to \mathrm{DY}/W^{\pm}/Z^0$:

$$f_{1T}^{\mathrm{SIDIS}}(x, k_T, Q^2) = -f_{1T}^{p+p\to \mathrm{DY}/W^{\pm}/Z^0}(x, k_T, Q^2). \quad (1)$$

This non-universality of the Sivers function is a fundamental prediction from the gauge invariance of QCD and is based on the QCD factorization formalism [36–38]. The experimental verification of this sign change hypothesis is a crucial measurement in hadronic physics and provides an important test of QCD factorization.

In transversely polarized p+p collisions, the Sivers function can be accessed through the transverse single spin asymmetry (TSSA) measurements in DY or $W^{\pm}/Z^0$ boson production. This asymmetry is generated from the correlation between the proton spin and the intrinsic k_T of a parton inside the proton. The amplitude of the TSSA (A_N) can be extracted from the ϕ modulation of $(\sigma_\uparrow - \sigma_\downarrow)/(\sigma_\uparrow + \sigma_\downarrow)$, where ϕ is the azimuthal angle of the measured particle and $\sigma_{\uparrow(\downarrow)}$ is its cross section with the spin direction of the proton oriented up (down) relative to the direction of its momentum.

In this Letter, we report the first measurement of the Z^0/γ^* differential cross section as a function of its p_T in p+p collisions at a center-of-

mass energy of 510[1] GeV by the STAR experiment. The measurement of the Z^0/γ^* total cross section is improved by adding a new data set compared with the previous result [39]. We also report the measurement of Z^0/γ^* A_N in transversely polarized p+p collisions at 510 GeV. These measurements are derived from studies of the $Z^0/\gamma^* \to e^+e^-$ decay channel for outgoing leptons at mid-rapidity (pseudorapidity $|\eta| < 1$).

2. Experiment and dataset

The STAR detector [40] comprises many separate subsystems, each with specific capabilities. An essential subsystem for this measurement is the time projection chamber (TPC) [41]. Together with a 0.5 T solenoidal magnetic field, the TPC provides charge discrimination and precision momentum measurements over a $|\eta| < 1.3$ range with full 2π azimuthal coverage. The barrel electromagnetic calorimeter (BEMC) [42] surrounding the TPC measures the energy deposited by energetic photons and electrons with $|\eta| < 1$ over the full azimuth. The Z^0 candidate events were recorded using a calorimeter trigger system which requires 12 GeV of transverse energy (E_T) in a $\Delta\eta \times \Delta\phi$ region of $\sim 0.1 \times 0.1$ of the BEMC. Primary vertices were reconstructed along the beam axis within 100 cm from the center of the STAR interaction region.

In this analysis, the differential cross section results[2] combined data samples collected in 2011, 2012, 2013, and 2017 with an integrated luminosity of 680 pb^{-1}. The A_N result was measured from the data sample collected in 2017 with transversely polarized proton beams. The integrated luminosity was 340 pb^{-1}, which is 14 times higher than the previously published results of A_N based on 2011 data [43]. The beam polarization was determined using Coulomb-nuclear interference proton-carbon polarimeters, calibrated with a polarized hydrogen gas-jet target [44]. The average beam polarization $\langle P \rangle$ for 2017 data was 56%, with a relative scale uncertainty of $\Delta P/P = 1.4\%$.

3. Analysis and results

Following exactly the same methods used in the previous measurements of Z^0 A_N [43], $Z^0/\gamma^* \to e^+e^-$ events were selected by requiring a pair of $e^\pm$ candidates with opposite charge sign, $|\eta^{lep}| < 1$, and $p_T^{lep} > 25$ GeV/c. In this analysis, we improved the measurement of the momentum of the electron and positron through scaling the angle measured by the TPC with its energy measured by the BEMC, instead of obtaining the momentum directly from the TPC. The invariant mass distribution of the e^+e^- pairs is shown in Fig. 1. A signal is observed near the invariant mass of the Z^0 at ~ 91 GeV/c^2. Background events, largely combinatorial in nature (uncorrelated $e^\pm$ pairs), were studied by requiring a pair of $e^\pm$ candidates with the same charge sign as shown in Fig. 1 with the open squares. The solid circles represent the mass distribution after combinatorial background subtraction.

The Z^0 candidates from e^+e^- were selected with a mass window cut of $73 < M_{e^+e^-} < 114$ GeV/c^2, the same cut as the earlier measurements [43]. The candidate's transverse momentum $p_T^{Z^0}$ was the vector sum of p_T^{lep} from the two decay leptons. The $p_T^{Z^0}$ distribution was corrected for three effects: combinatorial background contributions; p_T unfolding due to detector resolution; and the detector inefficiencies. The combinatorial background correction was applied by subtracting the geometric average of the p_T distribution of e^+e^+ and e^-e^- pairs within the mass window. The uncertainty due to this correction, estimated from the statistical uncertainties of the p_T distribution of e^+e^+ and e^-e^- pairs, was assigned as one of the systematic uncertainties to the final $p_T^{Z^0}$ spectrum.

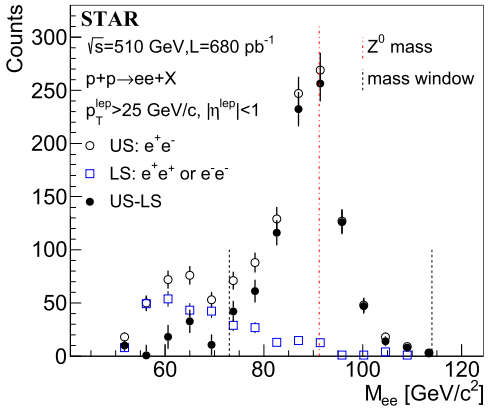

Fig. 1. The invariant mass distribution of the reconstructed lepton pairs at STAR. The open circles represent e^+e^- pairs by requiring the charges of two lepton candidates to have opposite signs. The open squares represent the like-sign pairs of e^+e^+ and e^-e^-. The solid circles represent the mass distribution after the combinatorial background subtraction. The vertical bars indicate the statistical uncertainties.

The detector effects on the $p_T^{Z^0}$ distribution were corrected by unfolding and efficiency corrections. Monte-Carlo samples generated by "Perugia 0" [45] tuned PYTHIA 6.4 [46] were used at the "particle level". The detector response for these samples was simulated using GEANT 3 [47], following which the simulated events were embedded into zero-bias p+p events and recorded with no cuts applied. The resulting event was at the "detector level". An iterative unfolding technique was performed using the RooUnfold package [48], with the unfolding matrix obtained from a one-to-one mapping between the particle- and the detector-level $p_T^{Z^0}$. The unfolding method was applied to eliminate the bin migration in $p_T^{Z^0}$ due to momentum resolution. The efficiency correction was then applied to the unfolded $p_T^{Z^0}$ distribution. The detector efficiency, bin by bin in $p_T^{Z^0}$ for each year's data, is defined as the number of reconstructed Z^0s after the cuts divided by the number of Z^0s from the Monte-Carlo generator level. The uncertainty of the detector efficiency correction was estimated from the statistical error of the simulated samples, which was taken as another source of systematic uncertainty of the $p_T^{Z^0}$ spectrum.

The differential cross section was measured in eleven $p_T^{Z^0}$ bins. Besides the contributions from the combinatorial background and efficiency corrections, the bin-by-bin systematic uncertainties were also estimated by varying the minimum p_T requirement of the decay leptons and the uncertainty on the calibration in energy measured by the BEMC. As described earlier, the decay lepton's p_T was required to be larger than 25 GeV/c. To estimate the uncertainty caused by this p_T cut, we varied the selection by requiring the lepton's p_T to be larger than 24 and 26 GeV/c. The relative difference of $p_T^{Z^0}$ distribution, from the various selection cuts to the original one, was defined as the contribution of the p_T cut to the systematic uncertainty. The uncertainty of the BEMC calibration indicates how well the BEMC measures the lepton's energy. We varied the BEMC energy scale by changing the calibration gain by ± 5% for 2011–2013 data, the same as the published paper [39], and ± 3% for the 2017 data. The variation of the $p_T^{Z^0}$ distribution due to the gain changes was taken as the systematic uncertainty caused by the BEMC calibration uncertainty. Generally, the dominant systematic uncertainty comes from the BEMC calibration, which varies from 4% to 22% in different $p_T^{Z^0}$ bins. The systematic uncertainty caused by varying the minimum p_T cut is smaller than or around 3% for most of the $p_T^{Z^0}$ bins; at the highest p_T, it contributes 11% and 7% for $p_T^{\min} = 24$ and 26 GeV/c, respectively. The contributions to the systematic uncer-

[1] The cross section measurement was performed by the STAR experiment during the 2011, 2012, 2013, and 2017 p+p running periods at $\sqrt{s} = 500$ GeV (2011 data set) and 510 GeV (2012, 2013, and 2017 data sets). The center-of-mass energy correction of 2011 data set is estimated to be 0.2% for the combined data sets in cross section measurements, which has been ignored in this Letter.

[2] These cross section results were obtained by averaging appropriately over the beam polarizations.

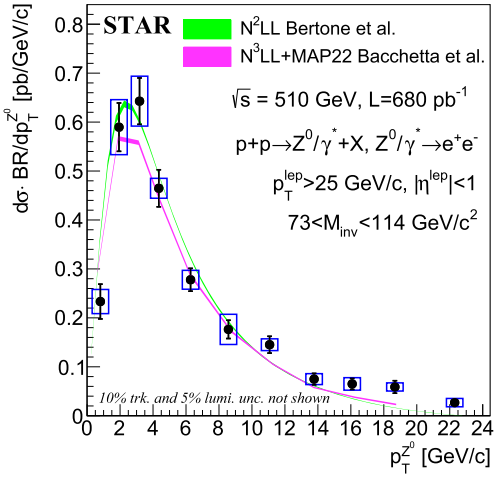

Fig. 2. The measured Z^0 cross section as a function of its p_{T}. The vertical bars indicate the statistical uncertainties and the vertical boxes indicate the systematic uncertainties. The horizontal width of the boxes is chosen for visual clarity and does not reflect the uncertainty in $p_{\mathrm{T}}^{Z^0}$. The p_{T}-independent uncertainties of 10% for Z^0 tracking efficiency and 5% for the luminosity are not included. The result is compared with perturbative predictions at the N^{2}LL [49] and N^{3}LL [50] accuracy.

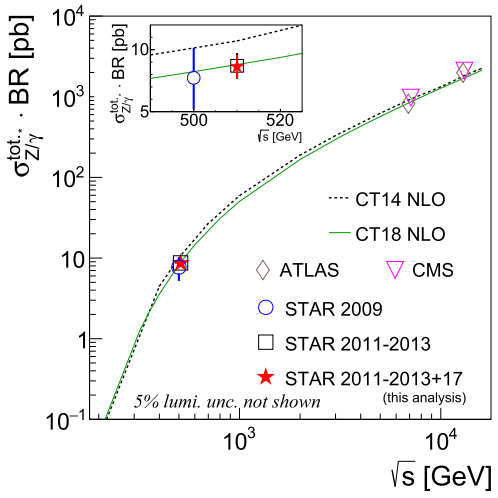

Fig. 3. The center-of-mass energy dependence of the total Z^0 cross section compared to CT14 [55] and CT18 [53] NLO PDF calculations. The measured value for the Z^0 total cross section in $\sqrt{s} = 510$ GeV p+p collisions is 8.63 ± 0.31 (stat) ± 0.31 (sys) ± 0.86 (eff) pb, based on a 2011–2013 and 2017 data sample with the integrated luminosity of 680 pb^{-1}. The uncertainty of 5% for the luminosity is not included in the figure. The previous STAR results [51,39] and higher energy results from the LHC [56,25,57,58] are shown as well. The vertical bars indicate the total uncertainties combining statistical and systematic ones. In the small panel, the previous and current STAR results are shown within a shorter range of collision energies.

tainty from the combinatorial background subtraction and efficiency corrections are relatively small as well, which are on average around 3% to 4% for all the $p_{\mathrm{T}}^{Z^0}$ bins. Detailed systematic uncertainties from each contribution can be found in Appendix A, Table A.2. Note, the p_{T}-independent uncertainties of 10% for Z^0 tracking efficiency and 5% for the luminosity are not included in the $p_{\mathrm{T}}^{Z^0}$ spectrum, but are included in the total cross section result.

After all the corrections and systematic uncertainty estimations described in the previous paragraphs are applied, the Z^0/γ^* cross section as a function of its p_{T} is obtained and shown in Fig. 2 for eleven p_{T} bins. Additionally, the Z^0/γ^* cross section as a function of its rapidity can be found in Appendix B, Fig. 5, providing more complementary information. BR is the branching ratio of $Z/\gamma^* \to e^+e^-$. The mean value of $p_{\mathrm{T}}^{Z^0}$ in each bin is plotted along the horizontal axis. The plotted symbols are explained in the figure caption. The measured p_{T}-differential cross section of the Z^0 provides an important input to constrain the energy scale dependence of TMDs. The data are compared to calculations by two different groups: V. Bertone et al. performed the calculation using the ζ-prescription and TMD evolution at the next-to-next-to-leading order logarithmic (N^{2}LL) accuracy in perturbative QCD [49]; A. Bacchetta et al. performed the calculation using the Monte Carlo replica method and resumming large logarithms at next-to-next-to-next-to-leading order logarithmic (N^{3}LL) accuracy [50]. Reference [49] did not include the Z^0 results from STAR, while reference [50] included a preliminary version of these results in their fit. Data are found to be consistent with the calculations from both groups. The low $p_{\mathrm{T}}^{Z^0}$ spectrum is of particular relevance, since the Q values should be high enough to safely apply factorization and, at the same time, $p_{\mathrm{T}}^{Z^0}$ should be much smaller than Q in order to apply the TMD formalism. This might explain the slight discrepancy between data and the TMD-based theoretical calculations at large values of $p_{\mathrm{T}}^{Z^0}$.

The Z^0 production cross sections were determined from the sample of events which satisfy the fiducial and kinematic requirements of this analysis. The total fiducial cross section can be obtained by integrating the differential cross section over $p_{\mathrm{T}}^{Z^0}$ from Fig. 2, and is $\sigma^{\mathrm{fid}}_{Z/\gamma^*} \cdot \mathrm{BR} = 2.76 \pm 0.10\ (\mathrm{stat}) \pm 0.10\ (\mathrm{sys})$ pb. To determine the total production cross sections $\sigma^{\mathrm{tot}}_{Z/\gamma^*}$, it is necessary to apply an acceptance correction factor, A_Z, in order to account for the fiducial and kinematic constraints imposed by the analysis. The total cross section can be written as

$$\sigma^{\mathrm{tot}}_{Z/\gamma^*} \cdot \mathrm{BR}(Z/\gamma^* \to e^+e^-) = \frac{\sigma^{\mathrm{fid}}_{Z/\gamma^*} \cdot \mathrm{BR}(Z/\gamma^* \to e^+e^-)}{A_Z}. \quad (2)$$

We applied the same method to calculate A_Z as done in [51,39] based on the FEWZ program [52], which provides perturbative QCD calculations for Z^0 production up to order N^{2}LO. We used the CT18 NLO PDF [53] as an input to obtain the value of A_Z, which is defined as the cross section ratio for the Z^0 boson with and without STAR acceptance cuts. Theoretical uncertainties in the calculation of this factor arise from several sources, including uncertainties within CT18 NLO PDF set and uncertainties on the strong coupling constant, α_s. The obtained A_Z is 0.32 ± 0.01. After the kinematic acceptance correction, the total Z^0 cross section from 2011–2013 and 2017 data is $\sigma^{\mathrm{tot}}_{Z/\gamma^*} \cdot \mathrm{BR} = 8.63 \pm 0.31\ (\mathrm{stat}) \pm 0.31\ (\mathrm{sys}) \pm 0.86\ (\mathrm{eff}) \pm 0.43\ (\mathrm{lumi})$ pb, with a relative uncertainty of 10% for the tracking efficiency based on the past Z^0 analysis [39] and 5% for the luminosity [54]. Compared to the published Z^0 results [51], the uncertainty of the tracking efficiency was updated based on a higher luminosity data set collected since 2011, which led to a higher uncertainty compared to the low luminosity data set from 2009. The luminosity calibration was improved by refining the accidentals correction on scalers, using beam position monitors instead of the magnet current set points utilized in [39] for the 2-dimensional beam displacement, and considering the intensity drop of the beam bunches, leading to a lower uncertainty of the luminosity compared to the previous value [39].

Fig. 3 shows the comparison of the total Z^0 cross section from this analysis with the published results from 2009 [51] and 2011–2013 [39] data from STAR, higher energy p+p data from the LHC [56,25,57,58], and two theoretical calculations based on CT14 and CT18 NLO PDFs [55,53]. The summary of the STAR results can be found in Table 1. In this analysis, 2011–2013 data have been reanalyzed using slightly different cuts on the Z^0 mass and the lepton's p_{T}, compared with [39]. The measured total Z^0 cross section from this analysis agrees with the previous 2009 and 2011–2013 results, as shown in the small panel inside Fig. 3. The statistical uncertainty in particular is improved significantly in this analysis compared to 2009 data. The systematic uncertainty increases in this analysis compared to the previous 2011–2013

Table 1
Total Z^0 cross section measured from different years' data at STAR.

Year	Ref	$\sigma^{tot.}_{Z/\gamma^*} \cdot \mathrm{BR} \pm stat_{unc.} \pm sys_{unc.} \pm \mathrm{lumi/eff}_{unc.}$ [pb]
2009	[51]	$7.7 \pm 2.1\ ^{+0.5}_{-0.9} \pm 1.0$ (lumi)
2011-2013	[39]	$8.7 \pm 0.5 \pm 0.1 \pm 0.9$ (eff) ± 0.8 (lumi)
2017	this analysis	$8.73 \pm 0.39 \pm 0.26 \pm 0.87$ (eff) ± 0.44 (lumi)
2011-2013+17	this analysis	$8.63 \pm 0.31 \pm 0.31 \pm 0.86$ (eff) ± 0.43 (lumi)

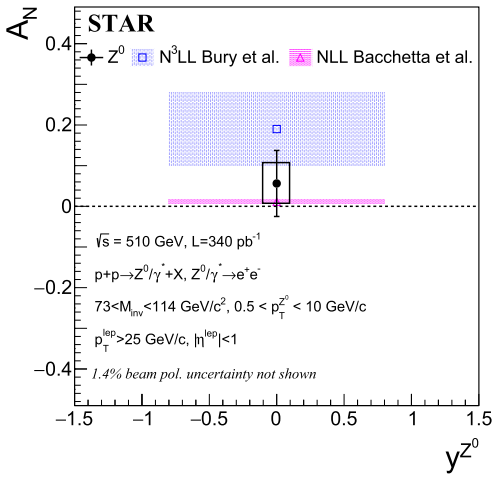

Fig. 4. The measured Z^0 transverse single spin asymmetry in transversely polarized p+p collisions, with an integrated luminosity of 340 pb^{-1}. The vertical bar indicates the statistical uncertainty and the vertical box indicates the systematic uncertainty. The result is compared with two theoretical calculations, both assuming the sign change hypothesis to be true. The blue band shows the theoretical calculation in the framework of TMD factorization at N^{3}LL accuracy [59,60]. The other theoretical calculation (pink band) is performed at NLL accuracy [61], in a fully consistent TMD framework. The horizontal width of the box and bands is chosen for visual clarity and does not reflect the uncertainty in y^{Z^0}.

result, since we considered extra contributions from the combinatorial background and efficiency corrections, and varying the minimum p_T requirement of the decay leptons, which were not taken into account in [39]. Additionally, a different implementation of the systematic uncertainty from the BEMC calibration was applied in this analysis. As the momentum of the decay lepton was reconstructed by scaling its energy from the BEMC, the effect of varying the BEMC gain on p_T migration is large. STAR data provides constraints on TMDs particularly at high x, since RHIC provides an intermediate collision energy. The ATLAS and CMS results measured at 7 and 13 TeV probe a region of x lower than the STAR data at 510 GeV. Therefore, the presented STAR results are complementary to the LHC results, and provide opportunities to investigate TMD evolution as a function of x. We also found all the data points to be in good agreement with the theoretical calculations.

In addition, we report the measured A_N of Z^0 production in $\sqrt{s} =$ 510 GeV p+p collisions at middle rapidity ($-1 < y^{Z^0} < 1$). The amplitude of the transverse single spin asymmetry of the Z^0, as described in Sec. 1, is extracted using the formula

$$A_N \cdot cos(\phi) = \frac{1}{\langle P \rangle} \cdot \frac{\sqrt{N_\uparrow(\phi) N_\downarrow(\phi+\pi)} - \sqrt{N_\uparrow(\phi+\pi) N_\downarrow(\phi)}}{\sqrt{N_\uparrow(\phi) N_\downarrow(\phi+\pi)} + \sqrt{N_\uparrow(\phi+\pi) N_\downarrow(\phi)}}, \quad (3)$$

where N is the yield of Z^0 reconstructed in collisions with an up/down ($\uparrow$ / $\downarrow$) beam polarization orientation. Defining the up transverse spin direction $\vec{S}_\perp$ along the y-axis and the direction of the incoming polarized beam $\hat{p}_{\mathrm{beam}}$ along the z-axis, the azimuthal angle is defined by $\vec{S}_\perp \cdot (\hat{p}_{\mathrm{beam}} \times \vec{p}_{\mathrm{T}}^{Z^0}) = |\vec{p}_{\mathrm{T}}^{Z^0}| \cdot \cos(\phi)$.

The result of A_N for the Z^0 is shown in Fig. 4, with detailed performance of cos(ϕ) fitting in Appendix C, Fig. 6. To study the TMD effects and test the sign change prediction, we limited $p_{\mathrm{T}}^{Z^0}$ to the range where the polarized TMD approach is applicable ($p_{\mathrm{T}} < 10$ GeV/c). In the figure, the vertical bar indicates the statistical uncertainty and the vertical box indicates the systematic uncertainty. The systematic uncertainty was estimated by measuring the A_N of all like-sign pairs, which was taken as a background asymmetry. The relative uncertainty of the averaged polarization was 1.4% and is not shown in the data point. The horizontal width of the box is chosen for visual clarity and does not reflect the uncertainty in y^{Z^0}.

This new result will provide critical input towards the extraction of the Sivers function, especially for valence quarks at relatively high x ($x \geq 0.1$). Two calculations from different groups are shown in Fig. 4, with both including the sign change hypothesis of the Sivers function. One is based on N^{3}LL accuracy of the TMD evolution in the collinear framework [59,60], in which, the Sivers function was expressed via an operator product expansion depending on the Qiu-Sterman function [62]. The other is calculated with NLL accuracy in the traditional TMD framework [61] and is based on the extractions of the unpolarized and Sivers functions in a fully consistent TMD framework, it shows similar results with [63]. Assuming no sign change simply flips the sign of each prediction to negative, maintaining the same magnitude. The current STAR result is not able to verify the sign change hypothesis, though it is slightly preferred over the non-sign change predictions.

4. Summary

We present the first measurement of the Z^0 cross section versus p_T in p+p collisions at $\sqrt{s} = 510$ GeV by the STAR experiment. The results combine all the data STAR has collected in 2011, 2012, 2013, and 2017, corresponding to a total luminosity of 680 pb^{-1}. The p_T spectrum of the Z^0, together with results from other experiments on DY, SIDIS, and Z^0, provide important constraints on the x and Q^2 evolution as well as the process dependence of the unpolarized TMDs. A high precision measurement of the Z^0 total cross section is also reported. When combined with data from higher energy collisions, it provides a stringent test of the energy dependence of PDFs.

We also present the measurement of the Z^0 A_N using transversely polarized p+p collision data collected in 2017, corresponding to an integrated luminosity of 340 pb^{-1}. The measured TSSA is 0.056 ± 0.081 (stat) ± 0.050 (sys). While the result can accommodate the sign change hypothesis that is based on the non-universality property of the Sivers function between DY/Z/W production and SIDIS, it cannot conclusively verify the prediction. Precision of the Z^0 cross section and A_N measurement will be improved using an additional 400 pb^{-1} sample of p+ p data at 508 GeV that STAR collected in 2022.

Declaration of competing interest

The authors declare that they have no known competing financial interests or personal relationships that could have appeared to influence the work reported in this paper.

Data availability

Data will be made available on request.

Acknowledgements

We thank the RHIC Operations Group and RCF at BNL, the NERSC Center at LBNL, and the Open Science Grid consortium for providing resources and support. This work was supported in part by the Office of Nuclear Physics within the U.S. DOE Office of Science, the U.S. National Science Foundation, National Natural Science Foundation of China, Chinese Academy of Science, the Ministry of Science and Technology of China and the Chinese Ministry of Education, the Higher Education Sprout Project by Ministry of Education at NCKU, the National Research

Foundation of Korea, Czech Science Foundation and Ministry of Education, Youth and Sports of the Czech Republic, Hungarian National Research, Development and Innovation Office, New National Excellency Programme of the Hungarian Ministry of Human Capacities, Department of Atomic Energy and Department of Science and Technology of the Government of India, the National Science Centre and WUT ID-UB of Poland, the Ministry of Science, Education and Sports of the Republic of Croatia, German Bundesministerium für Bildung, Wissenschaft, Forschung and Technologie (BMBF), Helmholtz Association, Ministry of Education, Culture, Sports, Science, and Technology (MEXT), Japan Society for the Promotion of Science (JSPS) and Agencia Nacional de Investigación y Desarrollo (ANID) of Chile.

Appendix A. Systematic uncertainties of Z^0 p_T spectrum

Table A.2
The relative systematic uncertainties (%) in each p_T bin from each source.

p_T bin	Like-sign correction	Eff. correction	min. p_T^{lep} 24 GeV/c	min. p_T^{lep} 26 GeV/c	BEMC gain
1	2.9	3.4	-0.003	-0.04	13.5
2	1.0	2.0	0.03	0.002	11.7
3	1.9	1.7	0.14	0.03	8.0
4	1.9	1.7	0.51	-0.08	4.0
5	2.2	1.5	0.07	0.11	7.5
6	2.7	1.9	1.2	-1.7	12.8
7	3.6	2.3	1.1	-3.5	6.4
8	6.1	2.7	0.88	-2.8	4.8
9	5.1	3.5	-1.1	0.72	16.4
10	7.5	5.6	4.8	-0.05	16.0
11	7.4	5.4	11.1	-6.8	22.0

Appendix B. Z^0/γ^* cross section as a function of its rapidity

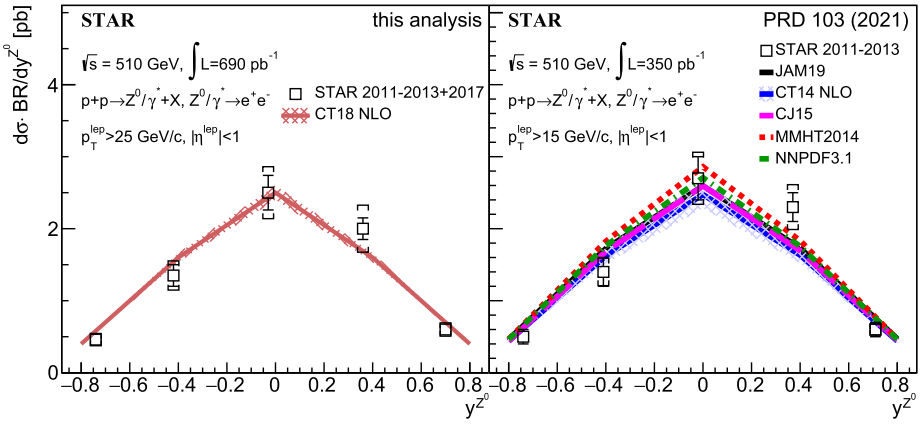

Fig. 5. Left: The measured Z^0/γ^* cross section as a function of its rapidity using datasets from 2011, 2012, 2013, and 2017. The data is compared with CT18 [53] NLO PDF calculation. Right: The previous STAR results from 2011–2013 datasets [39].

Appendix C. Cos fitting of the asymmetry from Eq. (4)

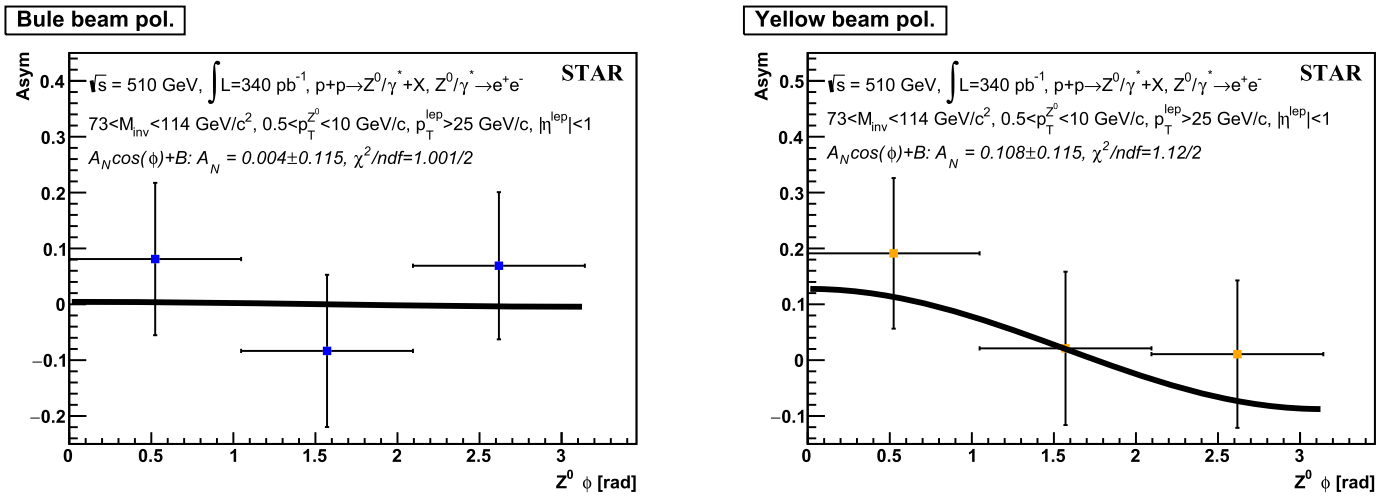

Fig. 6. The measured asymmetry of Z^0 as a function of its ϕ, with extraction of the A_N using cos fitting according to Eq. (4). Left: Blue beam is transversely polarized. Right: Yellow beam is transversely polarized. In each panel, the extracted A_N with its uncertainty can be found in the legend.

References

[1] D.E. Soper, Parton distribution functions, Nucl. Phys. B, Proc. Suppl. 53 (1997) 69–80, https://doi.org/10.1016/S0920-5632(96)00600-7, arXiv:hep-lat/9609018.

[2] S.M. Aybat, T.C. Rogers, TMD parton distribution and fragmentation functions with QCD evolution, Phys. Rev. D 83 (2011) 114042, https://doi.org/10.1103/PhysRevD.83.114042, arXiv:1101.5057.

[3] D. Sivers, Single-spin production asymmetries from the hard scattering of pointlike constituents, Phys. Rev. D 41 (1990) 83–90, https://doi.org/10.1103/PhysRevD.41.83, https://link.aps.org/doi/10.1103/PhysRevD.41.83.

[4] J.C. Collins, Fragmentation of transversely polarized quarks probed in transverse momentum distributions, Nucl. Phys. B 396 (1993) 161–182, https://doi.org/10.1016/0550-3213(93)90262-N, arXiv:hep-ph/9208213.

[5] S. Meissner, A. Metz, M. Schlegel, Generalized parton correlation functions for a spin-1/2 hadron, J. High Energy Phys. 08 (2009) 056, https://doi.org/10.1088/1126-6708/2009/08/056, arXiv:0906.5323.

[6] S.D. Drell, T.-M. Yan, Massive lepton pair production in hadron-hadron collisions at high-energies, Phys. Rev. Lett. 25 (1970) 316–320, https://doi.org/10.1103/PhysRevLett.25.316, Erratum: Phys. Rev. Lett. 25 (1970) 902.

[7] A. Airapetian, et al., Multiplicities of charged pions and kaons from semi-inclusive deep-inelastic scattering by the proton and the deuteron, Phys. Rev. D 87 (2013) 074029, https://doi.org/10.1103/PhysRevD.87.074029, arXiv:1212.5407.

[8] C. Adolph, et al., Hadron transverse momentum distributions in muon deep inelastic scattering at 160 GeV/c, Eur. Phys. J. C 73 (8) (2013) 2531, https://doi.org/10.1140/epjc/s10052-013-2531-6, Erratum: Eur. Phys. J. C 75 (2015) 94, arXiv:1305.7317.

[9] M. Aghasyan, et al., Transverse-momentum-dependent multiplicities of charged hadrons in muon-deuteron deep inelastic scattering, Phys. Rev. D 97 (3) (2018) 032006, https://doi.org/10.1103/PhysRevD.97.032006, arXiv:1709.07374.

[10] A.S. Ito, et al., Measurement of the continuum of dimuons produced in high-energy proton - nucleus collisions, Phys. Rev. D 23 (1981) 604–633, https://doi.org/10.1103/PhysRevD.23.604.

[11] G. Moreno, et al., Dimuon production in proton - copper collisions at $\sqrt{s}$ = 38.8 GeV, Phys. Rev. D 43 (1991) 2815–2836, https://doi.org/10.1103/PhysRevD.43.2815.

[12] P.L. McGaughey, et al., Cross-sections for the production of high mass muon pairs from 800-GeV proton bombardment of H-2, Phys. Rev. D 50 (1994) 3038–3045, https://doi.org/10.1103/PhysRevD.50.3038, Erratum: Phys. Rev. D 60 (1999) 119903.

[13] T. Affolder, et al., The transverse momentum and total cross section of e^+e^- pairs in the Z boson region from $p\bar{p}$ collisions at $\sqrt{s} = 1.8$ TeV, Phys. Rev. Lett. 84 (2000) 845–850, https://doi.org/10.1103/PhysRevLett.84.845, arXiv:hep-ex/0001021.

[14] A. Abulencia, et al., Measurements of inclusive W and Z cross sections in p anti-p collisions at $\sqrt{s}$ = 1.96 TeV, J. Phys. G 34 (2007) 2457–2544, https://doi.org/10.1088/0954-3899/34/12/001, arXiv:hep-ex/0508029.

[15] T. Aaltonen, et al., Transverse momentum cross section of e^+e^- pairs in the Z-boson region from $p\bar{p}$ collisions at $\sqrt{s} = 1.96$ TeV, Phys. Rev. D 86 (2012) 052010, https://doi.org/10.1103/PhysRevD.86.052010, arXiv:1207.7138.

[16] T. Aaltonen, et al., High-precision measurement of the W boson mass with the CDF II detector, Science 376 (6589) (2022) 170–176, https://doi.org/10.1126/science.abk1781.

[17] B. Abbott, et al., Measurement of the inclusive differential cross section for Z bosons as a function of transverse momentum in $\bar{p}p$ collisions at $\sqrt{s} = 1.8$ TeV, Phys. Rev. D 61 (2000) 032004, https://doi.org/10.1103/PhysRevD.61.032004, arXiv:hep-ex/9907009.

[18] V.M. Abazov, et al., Measurement of the shape of the boson transverse momentum distribution in $p\bar{p} \to Z/\gamma^* \to e^+e^- + X$ events produced at $\sqrt{s}$=1.96 TeV, Phys. Rev. Lett. 100 (2008) 102002, https://doi.org/10.1103/PhysRevLett.100.102002, arXiv:0712.0803.

[19] V.M. Abazov, et al., Measurement of the normalized $Z/\gamma^* -> \mu^+\mu^-$ transverse momentum distribution in $p\bar{p}$ collisions at $\sqrt{s} = 1.96$ TeV, Phys. Lett. B 693 (2010) 522–530, https://doi.org/10.1016/j.physletb.2010.09.012, arXiv:1006.0618.

[20] G. Aad, et al., Measurement of the Z/γ^* boson transverse momentum distribution in pp collisions at $\sqrt{s}$ = 7 TeV with the ATLAS detector, J. High Energy Phys. 09 (2014) 145, https://doi.org/10.1007/JHEP09(2014)145, arXiv:1406.3660.

[21] G. Aad, et al., Measurement of the transverse momentum and ϕ^*_η distributions of Drell–Yan lepton pairs in proton–proton collisions at $\sqrt{s} = 8$ TeV with the ATLAS detector, Eur. Phys. J. C 76 (5) (2016) 291, https://doi.org/10.1140/epjc/s10052-016-4070-4, arXiv:1512.02192.

[22] G. Aad, et al., Measurement of the transverse momentum distribution of Drell–Yan lepton pairs in proton–proton collisions at $\sqrt{s} = 13$ TeV with the ATLAS detector, Eur. Phys. J. C 80 (7) (2020) 616, https://doi.org/10.1140/epjc/s10052-020-8001-z, arXiv:1912.02844.

[23] S. Chatrchyan, et al., Measurement of the rapidity and transverse momentum distributions of Z bosons in pp collisions at $\sqrt{s} = 7$ TeV, Phys. Rev. D 85 (2012) 032002, https://doi.org/10.1103/PhysRevD.85.032002, arXiv:1110.4973.

[24] V. Khachatryan, et al., Measurement of the transverse momentum spectra of weak vector bosons produced in proton-proton collisions at $\sqrt{s} = 8$ TeV, J. High Energy Phys. 02 (2017) 096, https://doi.org/10.1007/JHEP02(2017)096, arXiv:1606.05864.

[25] A.M. Sirunyan, et al., Measurements of differential Z boson production cross sections in proton-proton collisions at $\sqrt{s}$ = 13 TeV, J. High Energy Phys. 12 (2019) 061, https://doi.org/10.1007/JHEP12(2019)061, arXiv:1909.04133.

[26] R. Aaij, et al., Measurement of forward W and Z boson production in pp collisions at $\sqrt{s} = 8$ TeV, J. High Energy Phys. 01 (2016) 155, https://doi.org/10.1007/JHEP01(2016)155, arXiv:1511.08039.

[27] R. Aaij, et al., Measurement of the forward Z boson production cross-section in pp collisions at $\sqrt{s} = 7$ TeV, J. High Energy Phys. 08 (2015) 039, https://doi.org/10.1007/JHEP08(2015)039, arXiv:1505.07024.

[28] R. Aaij, et al., Measurement of the forward Z boson production cross-section in pp collisions at $\sqrt{s} = 13$ TeV, J. High Energy Phys. 09 (2016) 136, https://doi.org/10.1007/JHEP09(2016)136, arXiv:1607.06495.

[29] M. Aghasyan, et al., First measurement of transverse-spin-dependent azimuthal asymmetries in the Drell-Yan process, Phys. Rev. Lett. 119 (11) (2017) 112002, https://doi.org/10.1103/PhysRevLett.119.112002, arXiv:1704.00488.

[30] C. Aidala, et al., Measurements of $\mu\mu$ pairs from open heavy flavor and Drell-Yan in $p + p$ collisions at $\sqrt{s} = 200$ GeV, Phys. Rev. D 99 (7) (2019) 072003, https://doi.org/10.1103/PhysRevD.99.072003, arXiv:1805.02448.

[31] D.W. Sivers, Single spin production asymmetries from the hard scattering of point-like constituents, Phys. Rev. D 41 (1990) 83, https://doi.org/10.1103/PhysRevD.41.83.

[32] D.W. Sivers, Hard scattering scaling laws for single spin production asymmetries, Phys. Rev. D 43 (1991) 261–263, https://doi.org/10.1103/PhysRevD.43.261.

[33] A. Bacchetta, M. Radici, Constraining quark angular momentum through semi-inclusive measurements, Phys. Rev. Lett. 107 (2011) 212001, https://doi.org/10.1103/PhysRevLett.107.212001, arXiv:1107.5755.

[34] M. Boglione, U. D'Alesio, C. Flore, J.O. Gonzalez-Hernandez, Assessing signals of TMD physics in SIDIS azimuthal asymmetries and in the extraction of the Sivers function, J. High Energy Phys. 07 (2018) 148, https://doi.org/10.1007/JHEP07(2018)148, arXiv:1806.10645.

[35] J. Cammarota, L. Gamberg, Z.-B. Kang, J.A. Miller, D. Pitonyak, A. Prokudin, T.C. Rogers, N. Sato, Origin of single transverse-spin asymmetries in high-energy collisions, Phys. Rev. D 102 (5) (2020) 054002, https://doi.org/10.1103/PhysRevD.102.054002, arXiv:2002.08384.

[36] J.C. Collins, Leading twist single transverse-spin asymmetries: Drell-Yan and deep inelastic scattering, Phys. Lett. B 536 (2002) 43–48, https://doi.org/10.1016/S0370-2693(02)01819-1, arXiv:hep-ph/0204004.

[37] S.J. Brodsky, D.S. Hwang, I. Schmidt, Initial state interactions and single spin asymmetries in Drell-Yan processes, Nucl. Phys. B 642 (2002) 344–356, https://doi.org/10.1016/S0550-3213(02)00617-X, arXiv:hep-ph/0206259.

[38] X.-d. Ji, F. Yuan, Parton distributions in light cone gauge: where are the final state interactions?, Phys. Lett. B 543 (2002) 66–72, https://doi.org/10.1016/S0370-2693(02)02384-5, arXiv:hep-ph/0206057.

[39] J. Adam, et al., Measurements of W and Z/γ^* cross sections and their ratios in p+p collisions at RHIC, Phys. Rev. D 103 (1) (2021) 012001, https://doi.org/10.1103/PhysRevD.103.012001, arXiv:2011.04708.

[40] K.H. Ackermann, et al., STAR detector overview, Nucl. Instrum. Meth. A 499 (2003) 624–632, https://doi.org/10.1016/S0168-9002(02)01960-5.

[41] M. Anderson, et al., The star time projection chamber: a unique tool for studying high multiplicity events at RHIC, Nucl. Instrum. Meth. A 499 (2003) 659–678, https://doi.org/10.1016/S0168-9002(02)01964-2, arXiv:nucl-ex/0301015.

[42] M. Beddo, et al., The STAR barrel electromagnetic calorimeter, Nucl. Instrum. Meth. A 499 (2003) 725–739, https://doi.org/10.1016/S0168-9002(02)01970-8.

[43] L. Adamczyk, et al., Measurement of the transverse single-spin asymmetry in $p^\uparrow + p \to W^\pm/Z^0$ at RHIC, Phys. Rev. Lett. 116 (13) (2016) 132301, https://doi.org/10.1103/PhysRevLett.116.132301, arXiv:1511.06003.

[44] O. Jinnouchi, et al., Measurement of the analyzing power of proton-carbon elastic scattering in the CNI region at RHIC, in: 16th International Spin Physics Symposium (SPIN 2004), World Scientific, Singapore, 2004, pp. 515–518.

[45] P.Z. Skands, Tuning Monte Carlo generators: the Perugia tunes, Phys. Rev. D 82 (2010) 074018, https://doi.org/10.1103/PhysRevD.82.074018, arXiv:1005.3457.

[46] T. Sjostrand, S. Mrenna, P.Z. Skands, PYTHIA 6.4 physics and manual, J. High Energy Phys. 05 (2006) 026, https://doi.org/10.1088/1126-6708/2006/05/026, arXiv:hep-ph/0603175.

[47] R. Brun, F. Bruyant, F. Carminati, S. Giani, M. Maire, A. McPherson, G. Patrick, L. Urban, GEANT detector description and simulation tool, https://doi.org/10.17181/CERN.MUHF.DMJ1, 10 1994.

[48] T. Adye, Unfolding algorithms and tests using RooUnfold, in: PHYSTAT 2011, CERN, Geneva, 2011, pp. 313–318, arXiv:1105.1160.

[49] V. Bertone, I. Scimemi, A. Vladimirov, Extraction of unpolarized quark transverse momentum dependent parton distributions from Drell-Yan/Z-boson production, J. High Energy Phys. 06 (2019) 028, https://doi.org/10.1007/JHEP06(2019)028, arXiv:1902.08474.

[50] A. Bacchetta, V. Bertone, C. Bissolotti, G. Bozzi, M. Cerutti, F. Piacenza, M. Radici, A. Signori, Unpolarized transverse momentum distributions from a global fit of Drell-Yan and semi-inclusive deep-inelastic scattering data, J. High Energy Phys. 10 (2022) 127, https://doi.org/10.1007/JHEP10(2022)127, arXiv:2206.07598.

[51] L. Adamczyk, et al., Measurement of the $W \to e\nu$ and $Z/\gamma^* \to e^+e^-$ production cross sections at mid-rapidity in proton-proton collisions at $\sqrt{s} = 500$ GeV, Phys. Rev. D 85 (2012) 092010, https://doi.org/10.1103/PhysRevD.85.092010, arXiv:1112.2980.

[52] Y. Li, F. Petriello, Combining QCD and electroweak corrections to dilepton production in FEWZ, Phys. Rev. D 86 (2012) 094034, https://doi.org/10.1103/PhysRevD.86.094034, arXiv:1208.5967.

[53] T.-J. Hou, et al., New CTEQ global analysis of quantum chromodynamics with high-precision data from the LHC, Phys. Rev. D 103 (1) (2021) 014013, https://doi.org/10.1103/PhysRevD.103.014013, arXiv:1912.10053.

[54] Offline analysis of luminosity calibration for $p+p$ 510 GeV data collected by the STAR experiment, 2023.

[55] S. Dulat, T.-J. Hou, J. Gao, M. Guzzi, J. Huston, P. Nadolsky, J. Pumplin, C. Schmidt, D. Stump, C.P. Yuan, New parton distribution functions from a global analysis of quantum chromodynamics, Phys. Rev. D 93 (3) (2016) 033006, https://doi.org/10.1103/PhysRevD.93.033006, arXiv:1506.07443.

[56] V. Khachatryan, et al., Measurements of inclusive W and Z cross sections in pp collisions at $\sqrt{s} = 7$ TeV, J. High Energy Phys. 01 (2011) 080, https://doi.org/10.1007/JHEP01(2011)080, arXiv:1012.2466.

[57] G. Aad, et al., Measurement of the $W \to \ell\nu$ and $Z/\gamma^* \to \ell\ell$ production cross sections in proton-proton collisions at $\sqrt{s} = 7$ TeV with the ATLAS detector, J. High Energy Phys. 12 (2010) 060, https://doi.org/10.1007/JHEP12(2010)060, arXiv:1010.2130.

[58] G. Aad, et al., Measurement of $W^\pm$ and Z-boson production cross sections in pp collisions at $\sqrt{s} = 13$ TeV with the ATLAS detector, Phys. Lett. B 759 (2016) 601–621, https://doi.org/10.1016/j.physletb.2016.06.023, arXiv:1603.09222.

[59] M. Bury, A. Prokudin, A. Vladimirov, Extraction of the Sivers function from SIDIS, Drell-Yan, and $W^\pm/Z$ data at next-to-next-to-next-to leading order, Phys. Rev. Lett. 126 (11) (2021) 112002, https://doi.org/10.1103/PhysRevLett.126.112002, arXiv:2012.05135.

[60] M. Bury, A. Prokudin, A. Vladimirov, Extraction of the Sivers function from SIDIS, Drell-Yan, and $W^\pm/Z$ boson production data with TMD evolution, J. High Energy Phys. 05 (2021) 151, https://doi.org/10.1007/JHEP05(2021)151, arXiv:2103.03270.

[61] A. Bacchetta, F. Delcarro, C. Pisano, M. Radici, The 3-dimensional distribution of quarks in momentum space, Phys. Lett. B 827 (2022) 136961, https://doi.org/10.1016/j.physletb.2022.136961, arXiv:2004.14278.

[62] J.-w. Qiu, G.F. Sterman, Single transverse spin asymmetries, Phys. Rev. Lett. 67 (1991) 2264–2267, https://doi.org/10.1103/PhysRevLett.67.2264.

[63] M.G. Echevarria, Z.-B. Kang, J. Terry, Global analysis of the Sivers functions at NLO+NNLL in QCD, J. High Energy Phys. 01 (2021) 126, https://doi.org/10.1007/JHEP01(2021)126, arXiv:2009.10710.